J Musculoskelet Neuronal Interact 2014; 14(3):286-293

Original Article

Hylonome

Linearity and sex-specificity of impact force prediction during a fall onto the outstretched hand using a single-damper-model

C.E. Kawalilak[1], J.L. Lanovaz[1], J.D. Johnston[2], S.A. Kontulainen[1]

[1]College of Kinesiology, University of Saskatchewan, Canada;
[2]Department of Mechanical Engineering, College of Engineering, University of Saskatchewan, Canada

Abstract

Objectives: To assess the linearity and sex-specificity of damping coefficients used in a single-damper-model (SDM) when predicting impact forces during the worst-case falling scenario from fall heights up to 25 cm. **Methods:** Using 3-dimensional motion tracking and an integrated force plate, impact forces and impact velocities were assessed from 10 young adults (5 males; 5 females), falling from planted knees onto outstretched arms, from a random order of drop heights: 3, 5, 7, 10, 15, 20, and 25 cm. We assessed the linearity and sex-specificity between impact forces and impact velocities across all fall heights using analysis of variance linearity test and linear regression, respectively. Significance was accepted at $P<0.05$. **Results:** Association between impact forces and impact velocities up to 25 cm was linear ($P=0.02$). Damping coefficients appeared sex-specific (males: 627 Ns/m, $R^2=0.70$; females: 421 Ns/m; $R^2=0.81$; sex combined: 532 Ns/m, $R^2=0.61$). **Conclusions:** A linear damping coefficient used in the SDM proved valid for predicting impact forces from fall heights up to 25 cm. Results suggested the use of sex-specific damping coefficients when estimating impact force using the SDM and calculating the factor-of-risk for wrist fractures.

Keywords: Forward Fall, Impact Force, Factor-of-risk, Outstretched Arm, Single Damper Model (SDM)

Introduction

Fractures of the distal forearm are common in children and postmenopausal women[1-3]. Forearm or wrist fractures occur when the applied force on bone exceeds the bone's ability to resist this force (i.e., bone strength). The most common scenario for this fracture type results from impact loading during a fall onto the hand of the outstretched arm, which represents the worst-case falling scenario[4-10]. Previous *ex vivo* research has proposed that fracture risk (or factor-of-risk, ϕ)[11] can be determined using the ratio of the impact force (or load, N) to whole bone strength (e.g., failure load, N), with $\phi \geq 1$ signifying potential for fracture. Advances in skeletal imaging and finite element (FE) modeling[12-18] have permitted non-invasive estimates of bone strength (failure load, N) while mathematical models have been used to estimate impact force from falling (load, N). The primary mathematical models include: 1) single damper model (SDM); 2) two-mass, spring-damper; and 3) multiple element, spring-damper model. Although inferior to the advanced multicomponent spring-damper models, the SDM approach is commonly reported when estimating impact forces epidemiologically and factor-of-risk for forearm fracture using the worst-case falling scenario (i.e., falling onto an *outstretched or straightened arm*) (Table 1)[14,19-28].

The SDM approach predicts the impact force corresponding to the initial high frequency impact force peak observed in experimental forearm fall data (commonly referred to as F_{1max}) by multiplying a calculated impact velocity by an experimentally derived damping coefficient. This impact force is generally associated with the highest risk for fracture incidence. The impact velocity is typically defined using conservation of energy principles equating kinetic and potential energy equations which relate falling height to impact velocity[14,19,21-23,26-28]. The falling height is generally defined as the height of the body's center of mass, often estimated as half an individual's standing height. The velocity at

The authors have no conflict of interest.

Corresponding author: Chantal E. Kawalilak, MSc, College of Kinesiology, University of Saskatchewan, 87 Campus Drive, Saskatoon SK S7N 5B2 Canada
E-mail: chantal.kawalilak@usask.ca

Edited by: F. Rauch
Accepted 13 August 2014

Reference	Method of Determining: *Impact Force (N)*	Damper	'Fall Height' in Model	Method of Determining: *Bone Failure Load (N)*	Factor-of-Risk: Sample Size and Sex	Age Range (years)
Muller ME, Webber CE, Bouxsein ML. Osteoporosis International **2003**; 14: 345-352.	*Equation:* damper x impact velocity	670 Ns/m	½ donor height	Mechanical compression testing	18 F, 20 M (Cadavers)	53-97
Melton LJ III, Riggs BL, Van Lenthe GH, et al. Journal of Bone and Mineral Research **2007**; 22(9): 1442-1448.	*Equation:* damper x impact velocity	670 Ns/m height	½ standing	FEA[3]	248 F	41-99
Kirmani S, Christen D, Van Lenthe GH, et al. Journal of Bone and Mineral Research **2009**; 24(6): 1033-1042.	*Equation:* damper x impact velocity	*Not Specified*[1]	*Not Specified*	FEA[3]	70 F, 70 M	12-18
Dalzell N, Kaptoge S, Morris N, et al. Osteoporosis International **2009**; 20: 1683-1694.	*Equation:* damper x impact velocity	670 Ns/m	½ standing height	FEA[3]	74 F, 58 M	20-79
Melton LJ III, Christen D, Riggs BL, et al. Osteoporosis International **2010**; 21(7): 1161-1169.	*Equation:* damper x impact velocity	670 Ns/m	½ standing height	FEA[3]	100 F (forearm fracture); 105 F (controls)	56-71[4]
Macdonald HM, Nishiyama KK, Kang J, et al. Journal of Bone and Mineral Research **2011**; 26(1): 50-62.	*Equation:* damper x impact velocity	*Not Specified*[1]	½ standing height[2]	FEA[3]	441 F, 201 M	20-99 F, 20-89 M
Kazakia G, Burghardt A, Link TM, et al. Journal of Biomechanics **2011**; 44(2): 257-266.	*Equation:* damper x impact velocity	*Not Specified*[1]	*Not Specified*	FEA[3]	53 F	45-65
Nishiyama KK, Macdonald HM, Moore SA, et al. Journal of Bone and Mineral Research **2012**; 27(2): 273-282.	*Equation:* damper x impact velocity	*Not Specified*[1]	*Not Specified*	FEA[3]	212 F, 186 M	9-22
Hansen S, Brixen K, Gravholt C. Journal of Bone and Mineral Research **2012**; 27(8): 1794-1803.	*Equation:* damper x impact velocity	670 Ns/m	½ standing height	FEA[3]	32 M/F (Turner syndrome patients); 32 M/F (controls)[5]	20-61; 19-58
Patsch JM, Burghardt AJ, Yap SP, et al. Journal of Bone and Mineral Research **2013**; 28(2): 313-324	*Equation:* damper x impact velocity	550 Ns/m	½ standing height	FEA[3]	80 F	50-75
Hansen S, Shanbhogue V, Folkestad L, et al. Calcified Tissue International **2014**; 94:269-281.	*Equation:* damper x impact velocity	670 Ns/m	½ standing height	FEA[3]	263 F; 236 M	20-70+

[1] '*Not Specified*' - reference to the prediction equation in Chiu and Robinovitch (1998).
[2] '*Not Specified*' but calculated to be ½ standing height.
[3] High-Resolution Peripheral Quantitative Computed Tomography (HR-pQCT) based finite element analysis (FEA).
[4] Reported as Interquartile Range (IQR).
[5] No sex differentiation reported.

Table 1. Current literature using the simple damper model to predict impact force in order to estimate the factor-of-risk (impact force: bone failure load). Literature listed in chronological order.

impact can be defined as $\sqrt{[2{*}9.81\ m/s^2 * (falling\ height)]}$. The most commonly used damping coefficient (multiplied by the impact velocity to predict impact force) is the constant linear value of 670 Ns/m from Chiu and Robinovitch[4], which represents the wrist/palmar damper when combining males and females (Table 1). When separating the sexes, the damping coefficients were reported as 790 Ns/m and 550 Ns/m for males and females respectively[4]. These damping coefficients were validated to predict impact forces on the hand of the outstretched forearm using fall heights of 1, 3, and 5 cm [4]. It is unclear, however, if a constant linear damping coefficient is valid at higher fall heights. The linearity assumption is fundamental when a constant damping co-efficient is used to estimate impact forces from standing height falls. Nonlinearity in

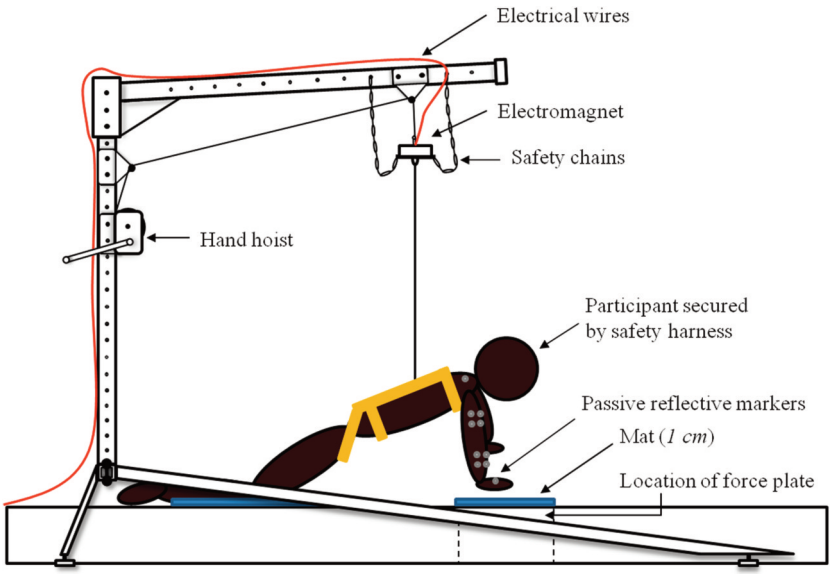

Figure 1. Experimental set-up of the fall-release apparatus and fall scenario. The participant's torso is supported using an industrial fall-restraint harness tethered to the fall-release apparatus via an electromagnet. Using the hand hoist, the participant's torso is raised so that the outstretched arm is at the pre-defined fall height directly over the force plate. The electromagnet is randomly timed to release the participant into a free-fall towards the force plate. Foam mats (1 cm height) provide additional padding for knees and palms of hands. Kinematics of the arm and hand are recorded using a 3D motion capture system (not illustrated).

the damping coefficient would lead to over- or under-estimation of impact force which would misguide fracture risk assessment and treatment options.

Our primary objective was to determine whether the association between impact force and impact velocity (i.e., damping coefficient) was linear across fall heights from 3 cm to 25 cm. We hypothesized that the linear assumption in the force-velocity relationship would justify usage of the constant damping coefficient in the SDM. Our secondary objective was to assess whether experimental data, with higher fall heights, would support usage of sex-specific damping coefficients in the SDM.

Methods

Participants

We recruited a convenient sample of 10 (5 males, 5 females) healthy adults (mean age (SD): 26 (4) years) to participate in the study. Participant average height was 169.5 (SD 9.5) cm; males were 177.3 (SD 4.6) cm and females were 161.6 (SD 5.2) cm. The average mass was 74.0 (SD 14.3) kg; males were 84.5 (SD 11.5) kg and females were 63.5 (SD 7.4) kg. Participants were included in the study if they had no arm or wrist fracture in the past 2 years, if they had no bone or other diseases that predisposed them to an increased likelihood of fracture, and if they had no shoulder or back injuries. The maximum mass capacity of the experimental apparatus is 130 kg, therefore any person exceeding that mass was not invited to participate. Participants identified their dominant arm to ensure safe landing. We did this for safety purposes as the bones of the dominant limb are reported to be stronger than those of the non-dominant limb in both unilaterally trained athletes and non-athletic individuals[29-31]. These aforementioned issues were addressed by asking the participants to fill out a short questionnaire prior to their participation in the study. Pertaining to handedness, the questionnaire asked participants to identify the hand they write with. Participant consent was attained prior to any involvement in the study. This study was approved by the University of Saskatchewan Biomedical Research Ethics Board.

Anthropometry

Participant height, without shoes, was measured using a wall mounted stadiometer (Holtain Limited, Crymych, UK) to the nearest 0.1cm. Participant mass, without shoes, was measured using a calibrated electronic scale (Toledo Scale Company, Thunder Bay, Ontario, Canada) to the nearest 0.1 kg.

Fall-release apparatus

The fall-release apparatus consisted of a steel support frame with hand hoist used to suspend the participant's trunk into the air. Participants were positioned with their dominant hand aligned directly over the center of the force plate (Figure 1). The force plate was covered with a 1 cm thick foam 'yoga' mat to reduce participant anxiety associated with falling. Participants were fitted into an industrial fall restraint harness and suspended above the ground via a cable and electromagnet. The mass of the harness was 3.7 kg. The electromagnet was secured to the steel frame of the fall-release apparatus.

Determination of fall height

To accurately determine the fall height for each participant, we used an eight camera commercial motion capture system (Vicon Nexus, Vicon Motion Systems, CO) to track and resolve the 3-dimensional coordinates of passive reflective markers located on the participant's body. Fall heights were determined by individually calculating the difference between the participant's hand and the top of the foam mat placed on the force plate. The passive reflective markers were 14mm in diameter and were secured to each participant using hypoallergenic 2-way tape. Motion data were captured at 200 Hz.

The following seven nominal drop heights were used: 3, 5, 7, 10, 15, 20, 25 cm. Four repetitions of each height were attempted for a maximum total of 28 trials per participant with the order of all trials randomized. Not all trials produced useable data, with approximately 25 trials per participant being included in the analysis. The drop heights of 3 and 5cm were chosen in order to make a comparison between the force data of this study and that reported in Chiu and Robinovitch (1998). The fall height of 25 cm was the maximum capacity of our apparatus.

Body positioning

Participants began on their knees, with their shins and the dorsal/superior surface of the foot in contact with the ground, holding their dominant hand and forearm outstretched in front of them directly over the force plate (Figure 1). The participant's right and left hands were staggered, with the non-dominant arm slightly bent and raised relative to the outstretched dominant arm similar to Chiu and Robinovitch (1998). The rationale for staggering the hands was so that the ground impact would first occur on the dominant hand, followed by the non-dominant hand. The participants were instructed to fully extend the elbow of their dominant arm during the fall and were asked to maintain this position during impact in order to simulate the worst-case falling scenario. In order to assess participant compliance with this instruction, passive reflective marker clusters were attached to each participant's forearm and upper arm as illustrated in Figure 1. Placement of the markers in these locations allowed us to calculate the elbow angle and assess compliance in maintaining an outstretched arm (the worst-case falling scenario) in all fall heights. Post-test comparison indicated no significant differences in the elbow angle across fall heights (average angle 2.9°, SD 4.3°). Prior to release of the electromagnet, the body line was monitored so that a straight line could be drawn from the knees to the shoulders of the participants. Careful attention to body position was made to ensure the trunk was in-line with the femur with no flexion at the hip.

Experimental fall procedure

The electromagnet that suspended the participant's trunk above the force plate was connected to a computer programmed to release the participant after a random delay ranging from 0.1-5 seconds. The only indication for the electromagnet release was a verbal cue, "ready?".

Impact force assessment

The force at impact was recorded using a force plate (OR6-7, AMTI, MA) embedded in the floor of the data collection platform so that the measuring surface of the force plate was flush with the floor. Force plate data were collected at 2000 Hz and filtered using a hardware low-pass anti-aliasing filter with a cut-off frequency of 1000 Hz. Using custom software (2006b, MathWorks; Natick, MS, USA), the peak impact force (F_{1max}) following impact was defined for each fall trail. The average peak impact force for all fall trials, for each corresponding fall height, was calculated for each participant.

Force profile

The experimental data resulted in a force profile with two peak forces: F_{1max} and F_{2max}. The first force was a high-frequency transient force (F_{1max}) that occurred approximately 38 ms after initial hand impact. F_{1max} was followed by a lower peak force (F_{2max}) as the rest of the body (which was in motion at wrist impact) decelerated, this resulted in the body's load being transmitted through the arm to the force plate[4,6,32] (Figure 2). F_{2max} was found to occur approximately 106 ms after ground impact. These observations of the force profiles are consistent with those reported by Chiu and Robinovitch (1998).

Impact velocity assessment

Using the motion capture data, custom software (Matlab; 2006b, MathWorks; Natick, MS, USA) was applied to calculate the vertical velocity of the hand. The velocity just prior to impact (as identified from the force plate data) was calculated for each fall trial for all participants. The average vertical impact velocity of all fall trails, for each corresponding fall height, was defined for each participant.

Mat adjustment

Although the 'yoga' mat (thickness 1 cm) that covered the force plate had small damping capacity (damping ratio=0.08), its inclusion did affect the resulting impact forces. To reflect loading conditions on a solid surface, we adjusted the force by accounting for the effect of the mat. We multiplied the mat's damping coefficient (75 Ns/m) by the velocity at each impact and added this value to the corresponding impact forces defined from force plate data: [F_{1max}+(75 Ns/m*trial impact velocity)]. Across all fall heights, this adjustment increased the impact force by an average of 18%. This approach was verified using in-house impact studies assessing impact forces with and without the mat, including impact drop tests of a) solid objects (e.g., 7 kg sphere) released from heights up to 25 cm; and b) drop tests of individuals (not part of the current study; n=5) from drop heights of 3, 5 and 7 cm.

Statistical analysis

We defined the damping coefficients as the slope of the regression line relating the mat-adjusted impact force with the velocity at impact (intercept: 0,0). We report the coefficient of determination (R^2) and the damping coefficient (force-velocity

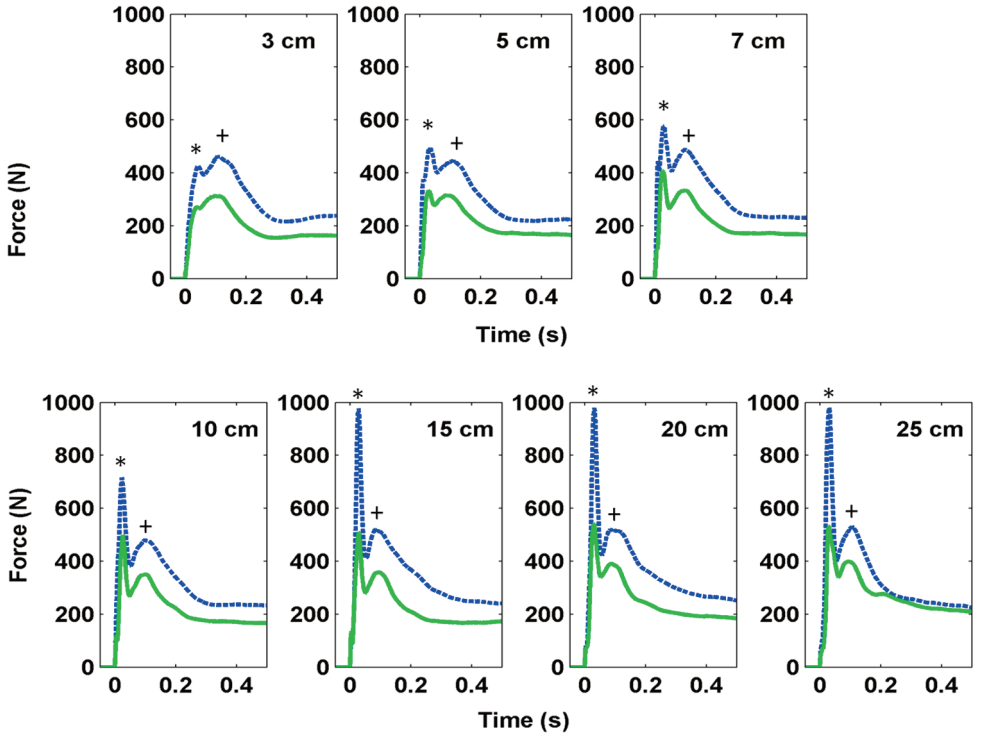

Figure 2. Experimental force (N) versus time (s) profile illustrating the initial peak (high-frequency transient force, F_{1max}; represented by '*') that occurred shortly after initial hand contact, followed by a second peak (lower in magnitude, F_{2max}; represented by '+') which is the force to decelerate the rest of the body mass. The blue (dashed) line represents the average male impact force at every fall height. The green (solid) line represents the average female impact force at every fall height. Time=0 at initial contact with the force plate.

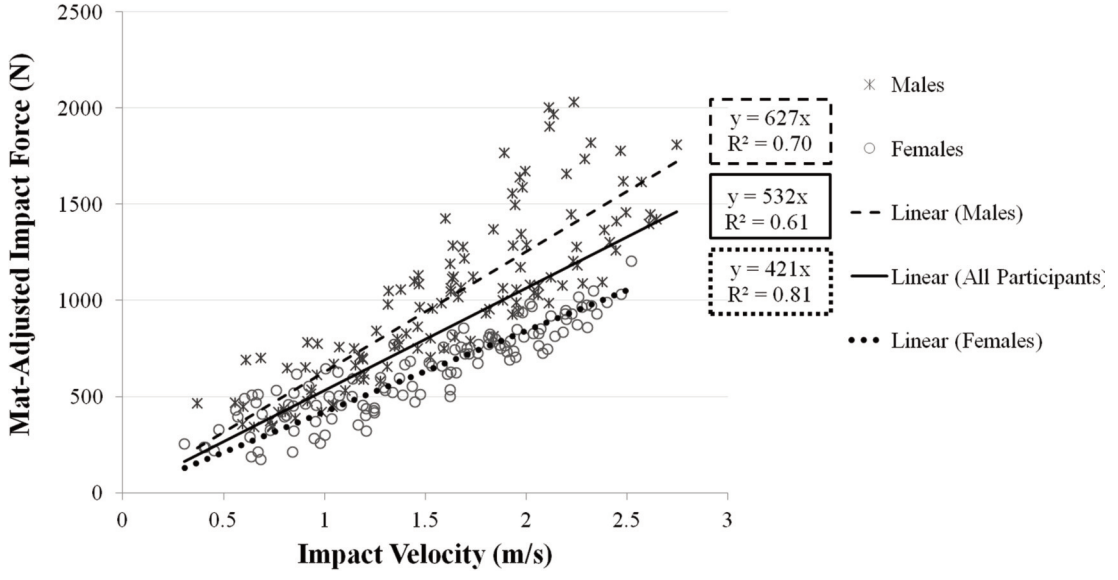

Figure 3. Impact force adjusted for the mat damper as a function of the impact velocity with increasing fall height. The star data points and dashed line represent the male data and associated regression equation with R^2. The circle data points and dotted line represent the female data and associated regression equation with R^2. The solid line and associated regression equation with R^2 correspond to the combined sexes.

slope) for all participants combined, as well as separately for the males and females. To ensure that an equal number of fall trials per sex were evaluated; we randomly matched the number of male and female trials for each fall height. For the first objective, we tested the linearity of the association between the mat-adjusted impact force and impact velocity across all fall heights using the analysis of variance (ANOVA) linearity and deviation from linearity tests. Significance was set to $P<0.05$. For the secondary objective, we assessed whether the fit (R^2) of the linear regression model between the impact velocities and forces across all fall heights improved when assessed separately for males and females versus for both sexes combined. All statistical analyses were performed using IBM SPSS commercial statistics software (PASW, Version 22 for Windows; SPSS Inc.; Chicago, IL, USA).

Results

The association between the mat-adjusted impact force and the impact velocity was linear across all fall heights (P_{linear}=0.02, R^2_{all}=0.61; $P_{non\text{-}linear}$=0.465) (Figure 3). The coefficient of determination (R^2) for the relationship between the mat-adjusted impact force and impact velocity (i.e., damping coefficients) appeared to improve when assessed separately for males (R^2_{males}=0.70, coefficient: 627 Ns/m) and females ($R^2_{females}$=0.81, 421 Ns/m) versus for both sexes combined (R^2_{all}=0.61, 532 Ns/m) (Figure 3).

Discussion

This was the first study to test whether the linear assumption of SDM for estimating the impact force during the worst-case falling scenario is valid at higher fall heights. Experimental data up to a fall height of 25 cm supported the linear relationship between impact velocities and forces. Our damping coefficients (sex combined: 532 Ns/m; males: 627 Ns/m; females: 421 Ns/m) from higher fall heights were comparable with previous research validating the SDM up to a fall height of 5cm (sex combined: 670 Ns/m; males: 790 Ns/m; females: 550 Ns/m)[4].

Our data indicated a different damping coefficient for males and females when estimating impact forces. This finding is supported by others[4,33]. Despite these findings, sex-specific damping coefficients have been rarely used when calculating the factor-of-risk for distal forearm fractures in the literature (Table 1). When estimating fracture risk, FE modeling can provide an approximation for bone strength (*numerator*) and models using a constant sex-specific damping coefficient (i.e., SDM; *denominator*) can provide an estimate of the impact forces during a fall onto the outstretched forearm. It is important to use sex-specific damping coefficients in these impact force prediction models because the commonly used general damping coefficient may overestimate fracture risk, especially in females - a population susceptible to osteoporotic fracture and most in need of accurate representation. The presentation of false positives in fracture risk assessment may subsequently lead to unnecessary treatment and exposure to detrimental side effects of anti-resorptive medications[34,35].

This study has strengths related to participant compliance in elbow angle and body positioning during the fall test trials. According to previous research[9], observed elbow angles in our trials (average 2.9º, SD 4.3º) indicated that participant arms' remained relatively straight (i.e., outstretched and stiff) during the testing procedure. This signifies that all participants were compliant with instructions to maintain an outstretched arm and facilitated the simulation of the worst-case falling scenario. Second, we paid careful attention to body position during each fall trial to ensure the trunk was in-line with the femur with no flexion at the hip. This ensured that the pivot point was at the knee which provided a more accurate measurement of free-fall impact forces when compared to a pivot point at the hip[36].

Study limitations relate to achievable fall heights, mat adjustment, participant age, and sample size. First, while we report fall data up to and including 25 cm, our maximum fall height represents less than one third of the estimated standing fall height of center of mass. The standing height of our participants was 1.77 m for males and 1.62 m for females, and the fall height associated with the impact velocity in the SDM has been estimated at half the standing height[19,14,21-23,26-28]. Although it would be ideal to measure the impact force at fall heights up to half the participant's standing height, it would increase the risk of injury. Several of our participants experienced post-test soreness in the palms of the hands, wrists, elbows and lower back. Higher fall heights would require the use of a thicker mat over the force plate to reduce participant anxiety associated with falling onto the outstretched hand. Using a mat, however, challenges the accurate estimation of the fall-related impact forces. A second limitation in our study relates to this damping effect of the thin yoga mat placed on top of the force plate. To reflect falling conditions on a solid surface, we adjusted the measured impact forces using methods verified from drop testing, with and without the mat, by dropping solid objects up to 25 cm and releasing five individuals from drop heights of 3, 5 and 7 cm. Although the adjusted forces may not perfectly reflect loading conditions on a solid surface, the linear SDM assumption was valid with and without mat adjustment (results not shown). Third, due to safety precautions we recruited young adult males and females for drop testing. It would be advantageous to determine how the damping coefficient changes with age as available damping coefficients are derived from young adult males and females[4]. Fourth, we assessed the data from a small sample of males and females. It would be prudent to cross-validate the models with new damping coefficients in a larger sample.

Summary

We investigated whether the association between impact force and impact velocity (i.e., damping coefficient) was linear across fall heights from 3 cm to 25 cm. We observed a linear association between the mat-adjusted impact force and impact velocity up to 25 cm. These results suggest that the linear SDM is valid up to 25 cm. Our secondary objective was to assess

the sex-specificity of the damping coefficients used in the SDM. Experimental data supported the use of sex-specific damping coefficients for males (627 Ns/m) and females (421 Ns/m) in the SDM when determining the factor-of-risk for distal forearm fractures.

Acknowledgement

We would like to thank all volunteers in this study and acknowledge Devin Glennie, Jon Aydt, and Yi Liu for their contributions in developing and constructing the fall-release apparatus. We would like to thank David Kobylak for his assistance in data collection and acknowledge the financial support from CIHR-RPP New Investigator Award (SK). Chantal Kawalilak acknowledges Canadian Institutes of Health Research (CIHR) Frederick Banting and Charles Best Canada Graduate Scholarships for financial support with her Master of Science research.

References

1. Johnell O, Kanis JA. An estimate of the worldwide prevalence and disability associated with osteoporotic fractures. Osteoporos Int 2006;17(12):1726-33.
2. Landin LA. Epidemiology of children's fractures. J Pediatr Orthop 1997;6:79-83.
3. Farr JN, Amin S, Melton LJ 3rd, Kirmani S, McCready LK, Atkinson EJ, Muller R, Khosla S. Bone strength and structural deficits in children and adolescents with a distal forearm fracture resulting from mild trauma. J Bone Miner Res 2014;29(3):590-9.
4. Chiu J, Robinovitch SN. Prediction of upper extremity impact forces during falls on the outstretched hand. J Biomech 1998;31:1169-76.
5. Burkhart TA, Andrews DM. Activation level of extensor carpi ulnaris affects wrist and elbow acceleration responses following simulated forward falls. J Electromyogr Kinesiol 2010; 20(6):1203-1210.
6. Chou P-H, Chou Y-L, Lin C-J, Su F-C, Lou S-Z, Lin C-F, Huang G-F. Effect of elbow flexion on upper extremity impact forces during a fall. Clinical Biomechanics 2001; 16:888-94.
7. DeGoede KM, Ashton-Miller JA. Fall arrest strategy affects peak hand impact force in a forward fall. J Biomech 2002;35(843-848):843.
8. DeGoede KM, Ashton-Miller JA. Biomechanical simulations of forward fall arrests: effects of upper extremity arrest strategy, gender and aging-related declines in muscle strength. J Biomech 2003;36(3):413-20.
9. DeGoede KM, Ashton-Miller JA Effect of elbow angle and rotational velocity on impact force during a fall onto an outstretched hand. In: American Society of Biomechanics, Pittsburg, Pennsylvania, 1999.
10. Kim K-J, Ashton-Miller JA. Biomechanics of fall arrest using the upper extremity: age differences. Clin Biomech (Bristol, Avon) 2003;18(4):311-8.
11. Hayes WC, Piazza SJ, Zyssett PK. Biomechanics of fracture risk prediction of the hip and spine by quantitative computed tomography. Radiol Clin North Am 1991; 29(1):1-18.
12. Boutroy S, Van Rietbergen B, Sornay-Rendu E, Munoz F, Bouxsein ML, Delmas PD. Finite element analysis based on *in vivo* HR-pQCT images of the distal radius is associated with wrist fracture in postmenopausal women. J Bone Miner Res 2008; 23(3):392-9.
13. Macneil JA, Boyd SK. Bone strength at the distal radius can be estimated from high-resolution peripheral quantitative computed tomography and the finite element method. Bone 2008;42(6):1203-13.
14. Melton LJ 3rd, Riggs BL, van Lenthe GH, Achenbach SJ, Muller R, Bouxsein ML, Amin S, Atkinson EJ, Khosla S. Contribution of *in vivo* structural measurements and load/strength ratios to the determination of forearm fracture risk in postmenopausal women. J Bone Miner Res 2007;22(9):1442-8.
15. Nishiyama KK, Macdonald HM, Hanley DA, Boyd SK. Women with previous fragility fractures can be classified based on bone microarchitecture and finite element analysis measured with HR-pQCT. Osteoporos Int 2012; 24(5):1733-40.
16. Pistoia W, van Rietbergen B, Lochmuller EM, Lill CA, Eckstein F, Ruegsegger P. Estimation of distal radius failure load with micro-finite element analysis models based on three-dimensional peripheral quantitative computed tomography images. Bone 2002;30(6):842-8.
17. Varga P, Pahr DH, Baumbach S, Zysset PK. HR-pQCT based FE analysis of the most distal radius section provides an improved prediction of Colles' fracture load *in vitro*. Bone 2010;47(5):982-8.
18. Vilayphiou N, Boutroy S, Sornay-Rendu E, Van Rietbergen B, Munoz F, Delmas PD, Chapurlat R. Finite element analysis performed on radius and tibia HR-pQCT images and fragility fractures at all sites in postmenopausal women. Bone 2010;46(4):1030-7.
19. Muller ME, Webber CE, Bouxsein ML. Predicting the failure load of the distal radius. Osteoporos Int 2003; 14(4):345-52.
20. Kirmani S, Christen D, van Lenthe GH, Fischer PR, Bouxsein ML, McCready LK, Melton LJ 3rd, Riggs BL, Amin S, Muller R, Khosla S. Bone structure at the distal radius during adolescent growth. J Bone Miner Res 2009; 24(6):1033-42.
21. Dalzell N, Kaptoge S, Morris N, Berthier A, Koller B, Braak L, van Rietbergen B, Reeve J. Bone micro-architecture and determinants of strength in the radius and tibia: age-related changes in a population-based study of normal adults measured with high-resolution pQCT. Osteoporos Int 2009;20(10):1683-94.
22. Melton LJ 3rd, Christen D, Riggs BL, Achenbach SJ, Muller R, van Lenthe GH, Amin S, Atkinson EJ, Khosla S. Assessing forearm fracture risk in postmenopausal women. Osteoporos Int 2010;21(7):1161-9.
23. Macdonald HM, Nishiyama KK, Kang J, Hanley DA, Boyd SK. Age-related patterns of trabecular and cortical

bone loss differ between sexes and skeletal sites: a population-based HR-pQCT study. J Bone Miner Res 2011; 26(1):50-62.
24. Kazakia GJ, Burghardt AJ, Link TM, Majumdar S. Variations in morphological and biomechanical indices at the distal radius in subjects with identical BMD. J Biomech 2011;44(2):257-66.
25. Nishiyama KK, Macdonald HM, Moore SA, Fung T, Boyd SK, McKay HA. Cortical porosity is higher in boys compared with girls at the distal radius and distal tibia during pubertal growth: an HR-pQCT study. J Bone Miner Res 2012;27(2):273-82.
26. Hansen S, Brixen K, Gravholt CH. Compromised trabecular microarchitecture and lower finite element estimates of radius and tibia bone strength in adults with turner syndrome: a cross-sectional study using high-resolution-pQCT. J Bone Miner Res 2012;27(8):1794-803.
27. Patsch JM, Burghardt AJ, Yap SP, Baum T, Schwartz AV, Joseph GB, Link TM. Increased cortical porosity in type 2 diabetic postmenopausal women with fragility fractures. J Bone Miner Res 2013;28(2):313-24.
28. Hansen S, Shanbhogue V, Folkestad L, Nielsen MM, Brixen K. Bone Microarchitecture and Estimated Strength in 499 Adult Danish Women and Men: A Cross-Sectional, Population-Based High-Resolution Peripheral Quantitative Computed Tomographic Study on Peak Bone Structure. Calcif Tissue Int 2014;94:269-81.
29. Haapasalo H, Kontulainen SA, Sievanen H, Kannus P, Jarvinen M, Vuori I. Exercise induced bone gain is due to enlargement in bone size without a change in volumetric bone density: a peripheral quantitative computed tomography study of the upper arms of male tennis players. Bone 2000;27(3):351-7.
30. Kontulainen S, Sievanen H, Kannus P, Pasanen M, Vuori I. Effect of long-term impact-loading on mass, size, and estimated strength of humerus and radius of female racquet-sports players: a peripheral quantitative computed tomography study between young and old starters and controls. J Bone Miner Res 2003;18(2):352-9.
31. Ducher G, Courteix D, Meme S, Magni C, Viala JF, Benhamou CL. Bone geometry in response to long-term tennis playing and its relationship with muscle volume: a quantitative magnetic resonance imaging study in tennis players. Bone 2005;37(4):457-66.
32. Davidson PL, Mahar B, Chalmers DJ, Wilson BD. Impact modeling of gymnastic back handsprings and dive-rolls in children. J Appl Biomech 2005;21:115-28.
33. Lakie M, Walsh EG, Wright GW. Resonance at the wrist demonstrated by the use of a torque motor: an instrumental analysis of muscle tone in man. J Physiol 1984; 353:265-85.
34. Pazianas M, Cooper C, Ebetino FH, Russel RGG. Long term treatment with bisphosphonates and their safety in postmenopausal osteoporosis. Ther Clin Risk Manag 2010;6:325-43.
35. Brown JP, Morin S, Leslie W, Papaioannou A, Cheung AM, Davison KS, Goltzman D, Hanley DA, Hodsman A, Josse R, Jovaisas A, Juby A, Kaiser SM, Karaplis A, Kendler DL, Khan AA, Ngui D, Olszynski WP, Ste-Marie LG, Adachi JD. Bisphosphonates for treatment of osteoporosis: Expected benefits, potential harms and drug holidays. CFP 2014;60(4):324-33.
36. Lo J, Ashton-Miller JA. Effect of upper and lower extremity control strategies on predicted injury risk during simulated forward falls: a study in healthy young adults. J Biomech Eng 2008;130(4):041015.